Beitr. Phys. Atmosph., August 1996, p. 393–407
0005-8173/96/03 0393–15 $ 3.00/0

Cyclonic Activity in a Warmer Climate

By F. LUNKEIT[1], M. PONATER[2], R. SAUSEN[2], M. SOGALLA[3], U. ULBRICH[3] and M. WINDELBAND[4]

[1]Meteorologisches Institut der Universität Hamburg, Bundesstraße 55, 20146 Hamburg, Germany
[2]Deutsche Forschungsanstalt für Luft- und Raumfahrt (DLR), Institut für Physik der Atmosphäre, Oberpfaffenhofen, 82234 Weßling, Germany
[3]Institut für Geophysik und Meteorologie, Universität zu Köln, Kerpener Straße 13, 50923 Köln, Germany
[4]Max-Planck-Institut für Meteorologie, Bundesstraße 55, 20146 Hamburg, Germany

(Manuscript received March 21, 1996; accepted June 26, 1996)

Abstract

A coupled atmosphere-ocean general circulation model was used to investigate potential changes of cyclonic activity due to a transient rise of atmospheric greenhouse gas concentrations. Despite the coarse resolution (T21) of the atmospheric submodel, a consistent response shows up for boreal winter. Changes in the distributions of bandpass filtered geopotential height variance and changes of the three-dimensional mean temperature structure, in particular Eady growth rates at the upper troposphere and the lower troposphere, both indicate baroclinic activity changes in certain well-defined regions. The most prominent feature is an increase of storminess over the eastern North Atlantic and western Europe. Here, the intensification of the storm track is associated with an enhanced frequency of cyclones. The frequency of extreme events in windspeed as well as precipitation are also found to increase in these regions.

Zusammenfassung

Zyklonenaktivität in einem wärmeren Klima

Mittels eines gekoppelten Atmosphäre-Ozean Modells wurde untersucht, wie sich die Zyklonenaktivität bei steigendem Treibhausgasgehalt der Atmosphäre ändert. Trotz der groben horizontalen Auflösung (T21) der atmosphärischen Modellkomponente ergibt sich ein konsistentes Bild für den nordhemisphärischen Winter. Änderungen der Verteilung von hochfrequenten Geopotentialfluktuationen und der mittleren dreidimensionalen Temperaturstruktur (insbesondere der Eady-Wachstumsraten in der oberen und unteren Troposphäre) sprechen übereinstimmend für eine Änderung der baroklinen Aktivität in ganz bestimmten geographischen Regionen. Eine regionale Verstärkung der Sturmtätigkeit über dem östlichen Nordatlantik und Westeuropa ist das auffälligste Merkmal in den vorgestellten Ergebnissen. In dieser Region gehen Verstärkung des mittleren ‚storm tracks', Zunahme der Anzahl von Bodenzyklonen und häufigeres Auftreten hoher Windgeschwindigkeiten und intensiver Niederschläge in konsistenter Weise miteinander einher.

1 Introduction

Due to the anthropogenic emissions of several greenhouse gases and resulting feedbacks within the climate system, a significant temperature rise in the troposphere can be expected during the course of the next 50 to 100 years (Houghton et al., 1996). Among the many aspects related to this so called global warming, its potential effect on the frequency and intensity of (tropical and extratropical) storms is actively debated by scientists as well as by the non-scientific public. Far too often, however, the complex problem has been oversimplified for the sake of quick answers. For example, the German "Enquete Kommission zum Schutz der Erdatmosphäre des 11. Deutschen Bundestages" states in their third report (Deutscher Bundestag, 1991) that *"the increase in the global evaporation rate can considerably enhance regional weather systems and ... raise the frequency of extreme meteorological*

events". Statements like this have gradually created the impression that an increase in the number and the strength of extreme weather events can be expected almost everywhere.

It is true that a quantitative and consistent assessment of changes in storminess is of fundamental importance for considering climate change impacts. However, such an assessment is not easily carried out. The storm activity at some given location is determined by a complex interaction system involving several competing cause and effect relationships. In this paper we will consider the topic of storminess change in a broader sense in order to produce a consistent picture of the global changes and regional cyclonic activity in the mid-latitudes.

Global warming studies are generally based on the results of general circulation models (GCMs). It is necessary that we use GCM data for the approach as proposed in our paper. Only GCM data provide consistent three-dimensional data sets of relevant variables with time series long enough to allow reasonable statistical assessments, even if a noisy feature such as the local storm activity is considered. Long time series of observational data are available for surface parameters only, which limits the possibility of creating a comprehensive picture of the global climate change arising from greenhouse warming. On the other hand, even the most recent GCMs are associated with systematic errors, which have to be studied and understood, if a solid conclusion from the model results is to be achieved.

A review of the available GCM studies dealing with changes of storm activity in a warmer climate has been given recently by Hall et al. (1994). They named three features of the time mean atmospheric response to greenhouse warming that should be taken into account in order to understand the associated storminess response: In the lowest atmospheric levels the temperature rise is stronger at higher latitudes than at lower latitudes. This means a weakening of the zonal mean temperature gradient and, hence, the zonal mean baroclinicity. In the upper troposphere the largest warming occurs in the tropics, leading to an increase in baroclinicity at higher altitudes. Both effects are expected to counteract each other, and it is difficult to predict, which one will have the dominating influence on the mean storminess. Theoretical studies predicting a dominating influence of the low level temperature gradient (Held and O'Brien, 1992; Pavan, 1996) have not yet found convincing support from complex GCMs (e.g. Hall et al., 1996).

Another potential aspect is the fact that the warmer atmosphere will contain more water vapour. It has usually been taken for granted that moist effects will cause an intensification of mid-latitude storminess, due to the possibility of releasing latent heat from a larger reservoir within individual storms (Flohn et al., 1992). However, there is also some argument (e.g. Held, 1993) that the global energy balance in a warmer climate can be achieved by less frequent or less intense storms, as for warmer conditions the same amount of air mass will transport more latent energy poleward.

To clarify the problem outlined above, several GCM simulations have been analysed so far, which give an impression what kind of response is to be expected. Most of the available investigations consider northern hemisphere winter conditions, where the maximum transient eddy activity is organized along two bandlike horizontal patterns, usually called the North Pacific and the North Atlantic storm track, respectively. Stephenson and Held (1993) investigated output from a $2.5 \times CO_2$ scenario simulation run in the so-called 'time slice mode'. The lower boundary conditions were taken from a coupled transient ocean-atmosphere simulation (Manabe et al., 1991). They found a marked weakening of the transient eddies in the North Atlantic region, but not much of a change over the North Pacific. Siegmund (1990) and Hall et al. (1994) used data from two versions of an atmosphere/slab ocean GCM (Wilson and Mitchell, 1987; Mitchell et al., 1990) to compare storm track differences between a $2 \times CO_2$ and a control simulation. Again, transient eddy statistics were used for the analysis. Both studies agree in predicting a northward shift of the North Atlantic as well as the North Pacific storm track. Most striking in Hall et al.'s results is an eastward shift of storm activity in the Atlantic with a distinct intensification of eddy activity over northwestern Europe. This feature is totally absent in Siegmund (1990). A northward shift of the North Atlantic storm track is also noticed by König et al. (1993), who applied a method of individual cyclone counting on data from a transient coupled global warming simulation (Cubasch et al., 1992). König et al. note, moreover, some eastward shift of cyclone frequency along the Pacific storm track. Using a similar technique, Lambert (1995) finds little change with respect to the cyclone frequency distribution in the Canadian Climate Centre GCM with a slab ocean model below. Very recently, Carnell et al. (1996) investigated sea level pressure field variances and cyclone counts in a transient coupled atmosphere-ocean model (Murphy and Mitchell, 1995) at

the time of CO_2 doubling. They observe a downstream and, for the Atlantic, also a northward shift of the variances, while surface low counts give a northward shift for both storm tracks.

Even if in many of the previous studies certain common features can be noticed (in particular for the North Atlantic storm track), in general the results concerning regional changes of cyclonic activity have remained ambiguous. This is not surprising, as all the models used differ with respect to their physical parameterization schemes and their spatial resolution. Hence, the simulated control state (for present-day climate conditions) is different, which may have an influence on the climate response. In addition, some differences in the various results may be due to the specific diagnostics applied (see, e.g., Carnell et al., 1996). So far, the sensitivity of the results has only been checked with respect to the horizontal resolution dependence (Senior, 1995). It has to be realized that, with the exception of Carnell et al., all previous investigations have relied mainly on only one method to diagnose cyclonic activity. When only one method is used, however, the possibility of checking the consistency of the global warming response simulated by a model is not fully exploited.

In the present paper we will combine several diagnostic tools to work out a more comprehensive picture of the various aspects of anthropogenic changes in cyclonic activity, including the problem of estimating changes in the frequency of extreme events. The methods have been chosen in a way such that the three-dimensional large scale variables as well as local variables are analyzed in order to check their consistency. The data are taken directly from a transient greenhouse warming simulation with a fully global coupled atmosphere-ocean GCM, where the resolution of the atmospheric model is rather low (T21). As in most of the papers mentioned above we focus on changes in northern hemisphere winter for comparison purposes.

The model configuration basic to our analysis is explained in Section 2. This section also contains a description of the simulated change of time averaged variables as far as these are relevant for the change in storminess. Section 3 deals with the consistency of changes in transient eddy statistics with parameters that describe the baroclinicity of the large scale time mean flow. In Section 4 local statistics of cyclones and extreme events are presented and these results are discussed in relation to the results of Section 3. Section 5 gives our conclusions including a critical discussion and an outlook.

2 Global Warming Simulated by ECHAM2/OPYC

We investigate simulations performed with the global coupled atmosphere-ocean GCM ECHAM2/OPYC, which has been described in some detail by Lunkeit et al. (1996a). Here we restrict ourselves to a brief overview. The atmospheric part of the model is the spectral general circulation model ECHAM2 at T21 horizontal resolution. It contains a state of the art physical parameterization package (including the full hydrological cycle) and has been shown to give a reasonable climatology of the northern hemisphere winter storm tracks (Roeckner et al., 1992). The correlation between the regional storm track structure and the variability of the large scale flow on monthly time scales is also well represented (Ponater et al. 1994). The ocean component of the coupled model is the general circulation model OPYC described by Oberhuber (1993a, 1993b).

Two simulations were carried out: A 210 year Control integration for present-day conditions and a 100 year transient Scenario A greenhouse warming experiment (Lunkeit et al., 1996b). The simulated mean climate of Control is in good agreement with observations (Lunkeit et al., 1996a). For the Scenario A simulation, the greenhouse gas concentration increases according to the respective IPCC Scenario A, i.e. by about 1.3 % per year (Houghton et al., 1992). Relative to the Control run, the annual global mean temperature rises by about 2.8 K within the 100 years.

Considering the topic of the present paper, only a brief selection of the changes of the northern hemisphere winter (December to February; DJF) mean climate is discussed. Climate change is defined as the difference between the last ten years of the Scenario A simulation and the corresponding decade of the Control run. To estimate the statistical significance of the signal, the null hypothesis of identical means is checked by an univariate two sided t-test.

The large scale pattern and the magnitude of the temperature change as simulated by ECHAM2/OPYC is in close agreement with the results of similar experiments by other groups (e.g. Cubasch et al., 1992; Manabe et al., 1991; Murphy and Mitchell, 1995). Figure 1 shows the geographical distribution of the changes of the near surface (2 m) temperature for DJF. At almost every gridpoint, the changes are statistically significant (95 %). The dominant features are a strong warming over the Arctic and the distinct land-sea contrast of the

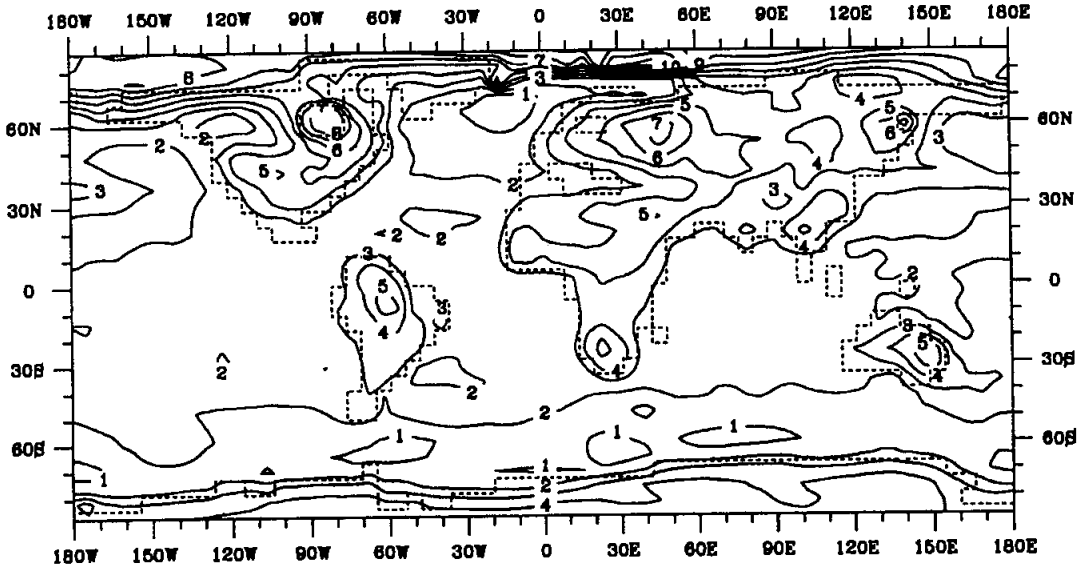

Figure 1 Geographical distribution of the change in near surface temperature. The change is defined as the difference between the time averaged last ten northern hemisphere winters of the Scenario A simulation and the corresponding years of the Control run. Units: K.

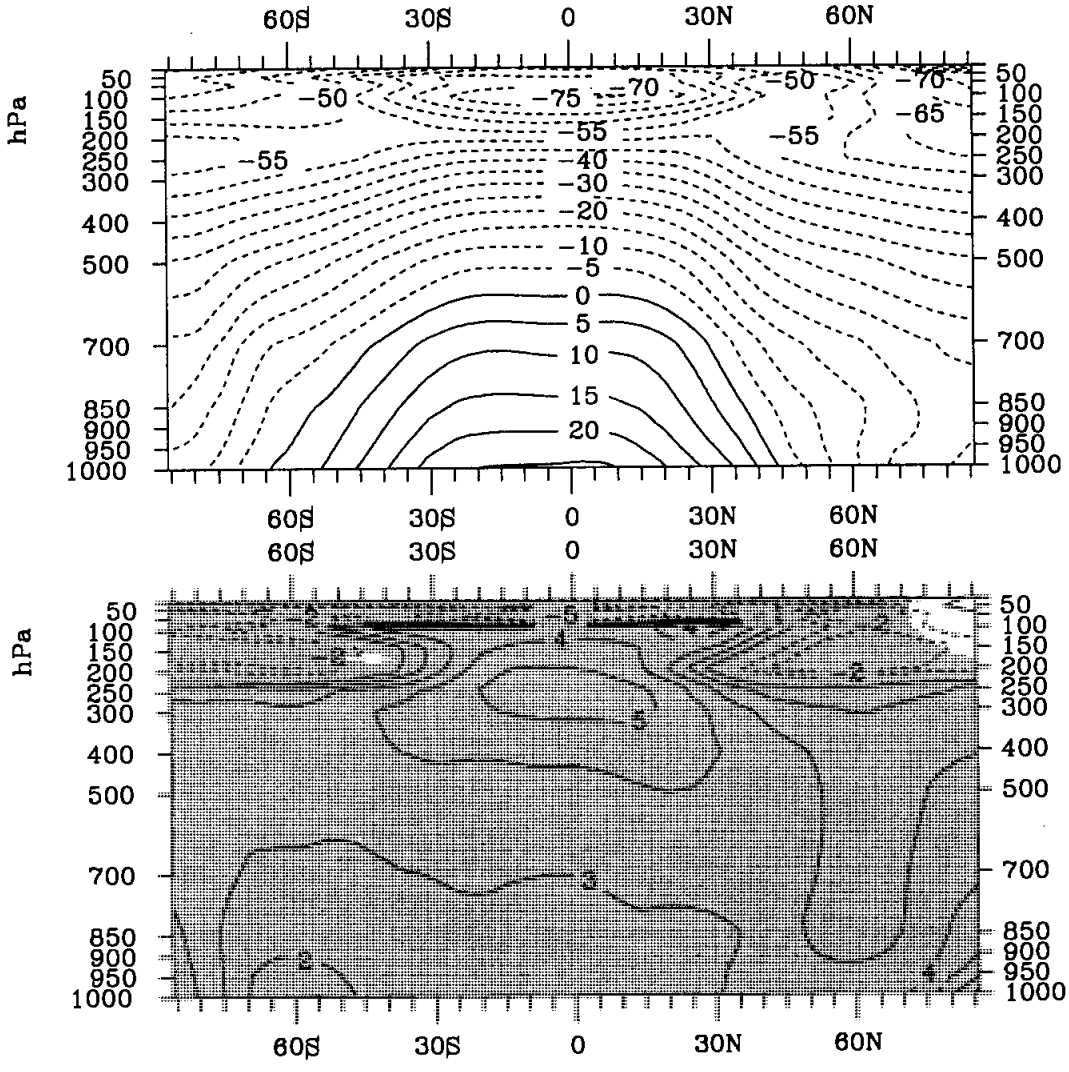

Figure 2 Vertical cross section of the zonally averaged temperature for the Control run (upper panel) and the difference between Scenario A and Control (lower panel). Shaded areas denote statistical significance on the 95 % level. Units: °C.

signals with enhanced warming over land. While the increases of temperature over central continental areas range up to 6 K, the anomalies are generally less than 3 K over the oceans. Consistent with other global warming simulations using coupled climate models, a minimum warming (0.5 K) is located southeast of Greenland.

The zonal mean temperature response of the atmosphere in the Scenario A experiment is shown in Figure 2. As for the near surface temperature, all changes are statistically significant at least on a 95 % level. The entire troposphere shows a warming with maximum values in the upper equatorial troposphere and at lower levels near the poles. The stratosphere, however, cools with largest values again occurring in the tropics. The related change of the zonal mean meridional temperature gradient is shown in Figure 3. The tropospheric gradient is enhanced in the northern hemisphere mid latitudes outside the boundary layer. The enhancement is most pronounced in the uppermost layers of the troposphere. The three-dimensional temperature response also implies changes of the mean dry static stability in the northern hemispheric mid-latitudes. This is demonstrated in Figure 4, which shows the zonal mean Brunt Vaisala frequency. The stability of the troposphere is reduced north of 40° North with maxima at the tropopause and, north of 60° North, close to the surface.

The zonal mean zonal wind (Figure 5) exhibits significant changes in the upper atmosphere reflecting the strengthening of the subtropical jetstream. Structure and amplitude of the zonal mean wind

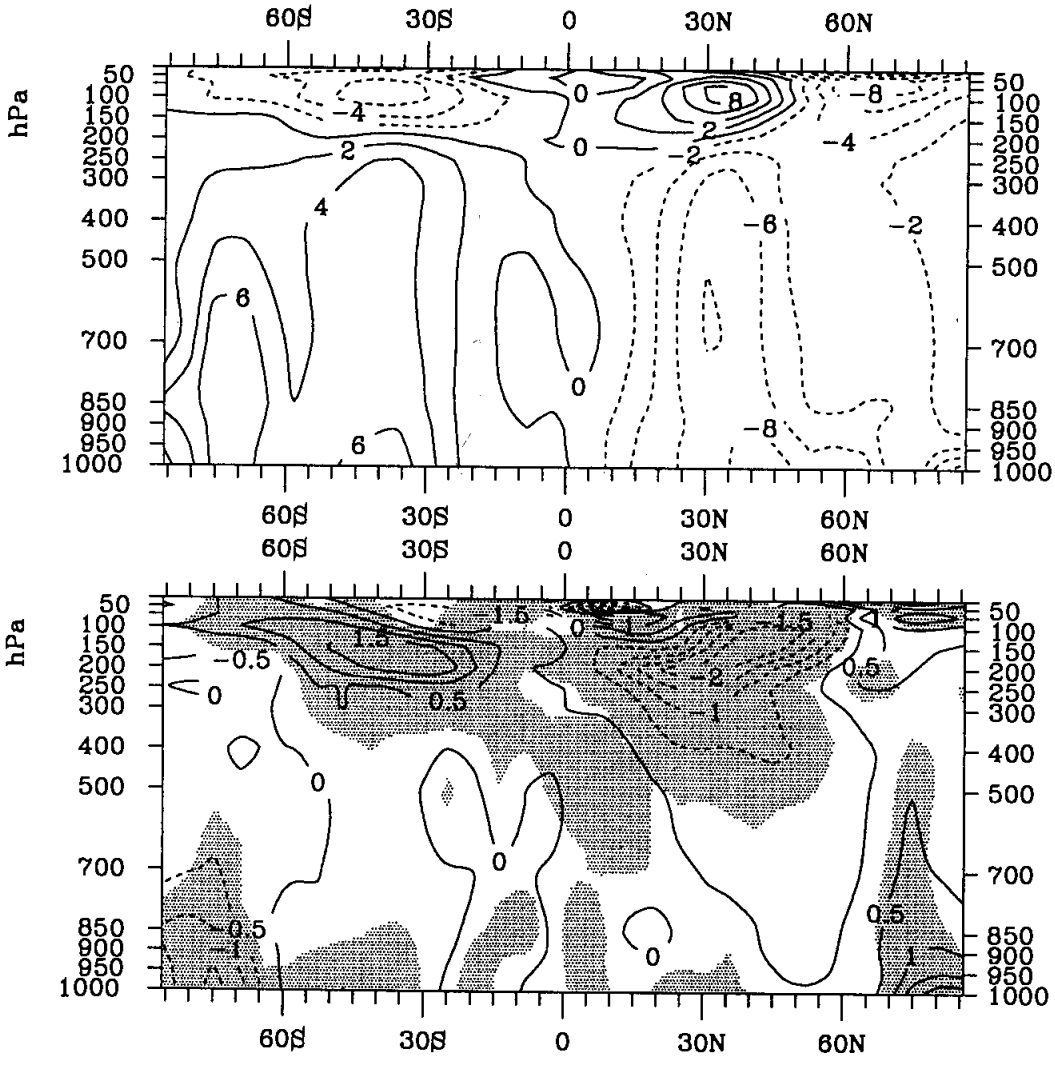

Figure 3 Vertical cross-section of the zonally averaged meridional temperature gradient for the Control run (upper panel) and the difference between Scenario A and Control (lower panel). Shaded areas denote statistical significance on the 95 % level. Units: K/1000 km. Isolines for the differences: ± 5, ± 2., ± 1.5, ± 1, ± 0.5, 0. [K/1000 km].

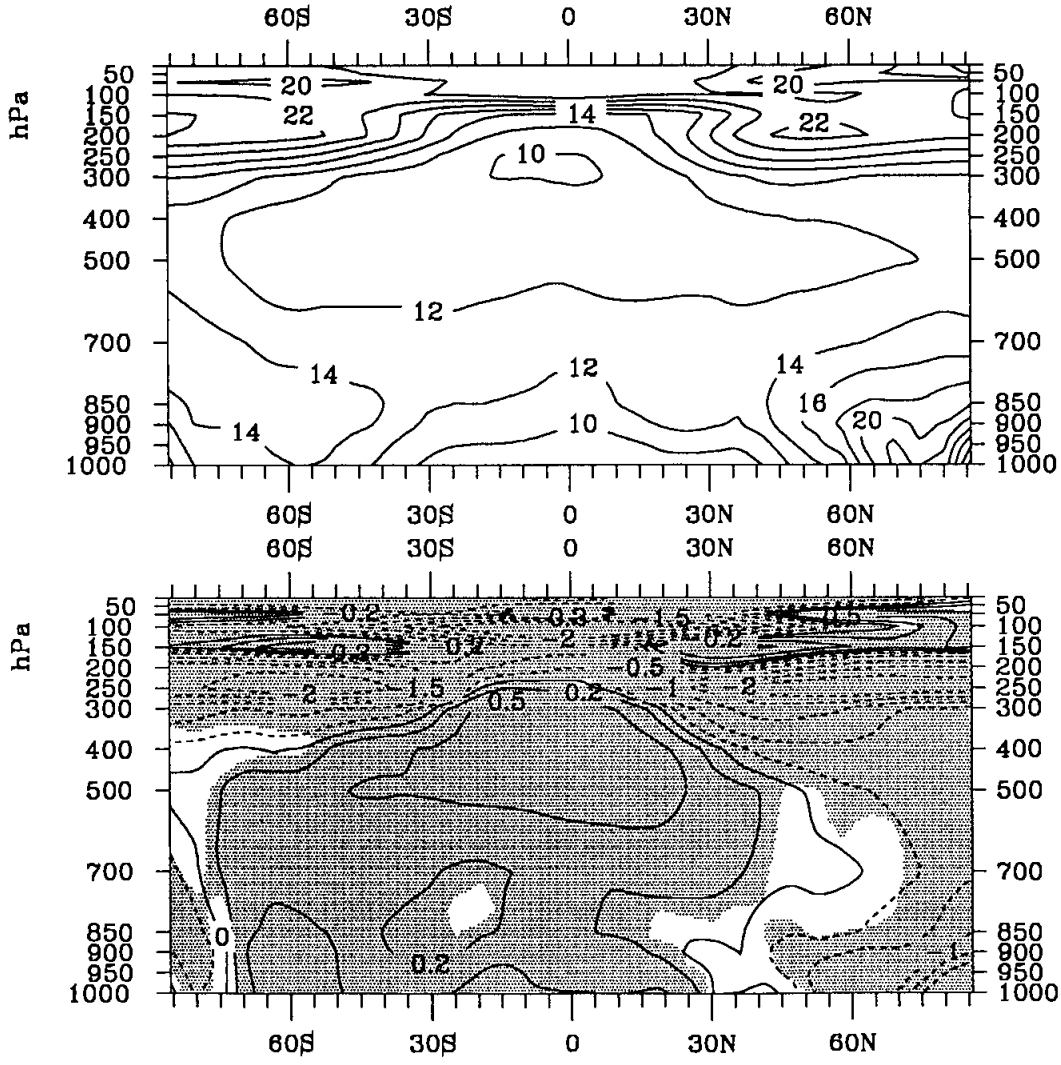

Figure 4 Vertical cross section of the zonally averaged Brunt Vaisala frequency for the Control run (upper panel) and the difference between Scenario A and Control (lower panel). Shaded areas denote statistical significance on the 95 % level. Units: 10^{-3}/s. Isolines for the differences: ± 5, ± 2, ± 1.5, ± 1, ± 0.5, ± 0.2, 0. [10^{-3}/s].

signal are similar as in Hall et al. (1994), but the jet increase is much stronger than that reported by Stephenson and Held (1993). In the lower troposphere only small and statistically insignificant changes can be noticed, connected with a strengthening and a northward shift of the northern hemispheric westerlies.

3 Storm Tracks and Baroclinicity

Regarding the changes of the zonal mean temperature and the related meridional and vertical temperature gradients, as discussed in the previous section, one could expect an overall increase of midlatitude transient eddy activity in the warmer climate. However, as both the distributions of northern hemispheric eddy activity and the warming signal are zonally asymmetric, three-dimensional structures have to be considered. A variable which comprises the influence of horizontal as well as vertical temperature gradients on eddy activity is the maximum Eady growth rate σ_{BI}. This measure of baroclinic instability can be defined as

$$\sigma_{BI} = 0.31 \frac{f}{N} \frac{\partial |v|}{\partial z} = -0.31 \frac{1}{T} \left(\frac{1}{g\theta} \frac{\partial \theta}{\partial z} \right)^{-\frac{1}{2}} |\nabla T| , \quad (1)$$

according to Lindzen and Farrel (1980). In Eq. (1), f denotes the Coriolis parameter, N the Brunt Vaisala frequency, g the gravitational acceleration, T the temperature, θ the potential temperature and v the horizontal velocity vector.

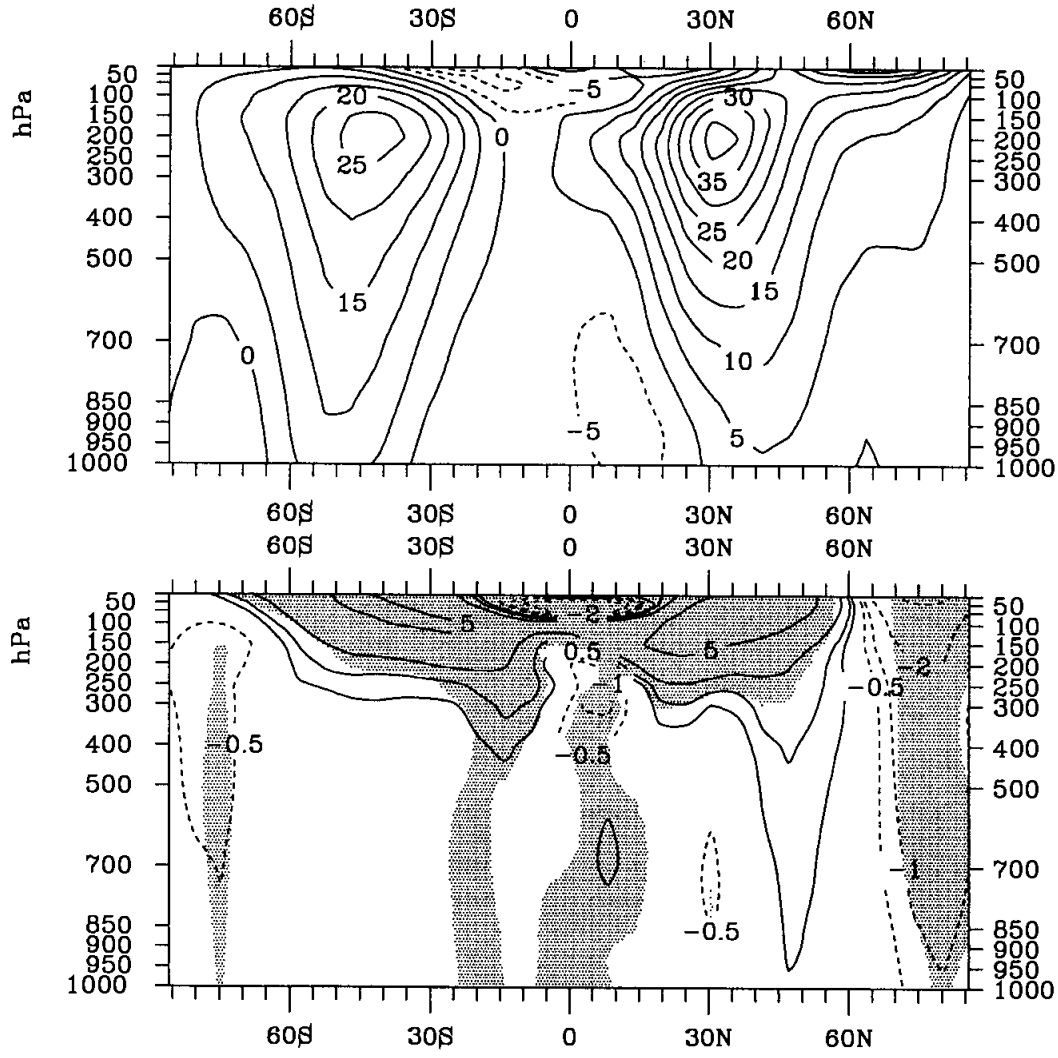

Figure 5 Vertical cross section of the zonally averaged zonal wind for the Control run (upper panel) and the difference between Scenario A and Control (lower panel). Shaded areas denote statistical significance on the 95 % level. Units: m/s. Isolines for the differences: ± 5, ± 2, ± 1, ± 0.5 [m/s].

Hoskins and Valdes (1990) have shown the climatological relation between σ_{BI} and the storm tracks based on observational data. This concept has also been applied to GCM simulations of anthropogenic changes (Hall et al., 1994) and with respect to conceptual simulations of storm track dynamics (Chang and Orlanski, 1993).

In the present study, the storm tracks were identified by the bandpass-filtered (Blackmon, 1976) variance of the geopotential height fields. Usually, this quantity has been analysed at a representative middle tropospheric level (500 hPa). However, in order to account for the specific vertical structure of the greenhouse signal, we consider an upper tropospheric (300 hPa), a middle tropospheric (500 hPa), and a near surface (1000 hPa) level. Likewise, the baroclinicity parameter (σ_{BI}) was computed separately for the upper troposphere (between 300 hPa and 400 hPa) and the lower troposphere (between 700 hPa and 850 hPa). Hence, we are able to assess the competitive effects from upper and lower level baroclinicity, though finer details within the vertical structure may be missed.

The climatological mean eddy activity simulated in the Control integration (Figure 6, left panel) is in reasonable agreement with observations. The storm tracks are correctly located, but the maximum values are underestimated, especially for the Atlantic storm track at upper levels. The maximum Eady growth rates of the model (Figure 6, right panel) show that the observed relation between regions of high growth rates and storm tracks (cf. Hoskins and Valdes, 1990) is also reproduced. Regions of large growth rates, where baroclinic waves potentially

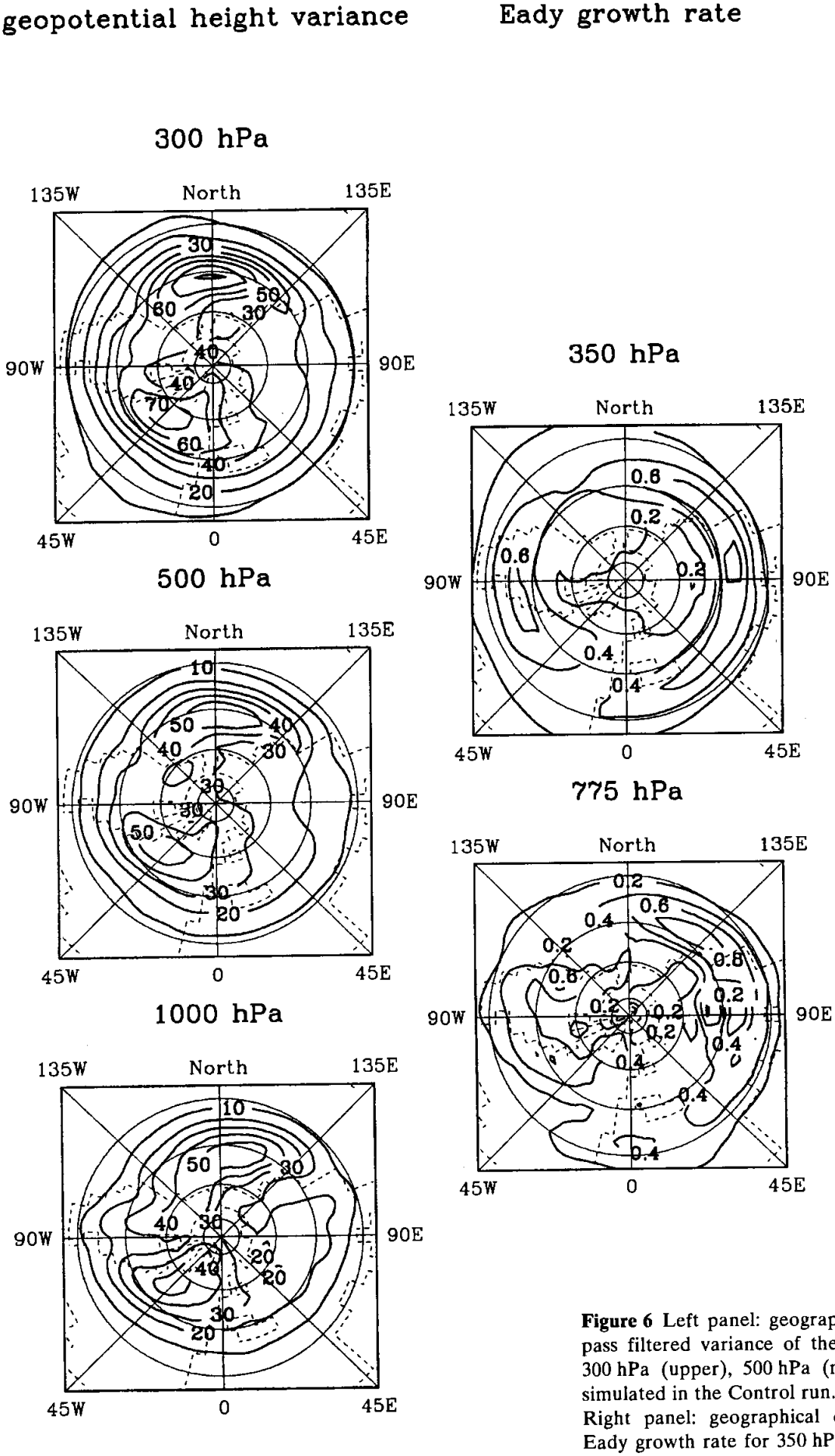

Figure 6 Left panel: geographical distribution of the band pass filtered variance of the geopotential height field for 300 hPa (upper), 500 hPa (middle) and 1000 hPa (lower) simulated in the Control run. Units: gpm.
Right panel: geographical distribution of the maximum Eady growth rate for 350 hPa (upper) and 775 hPa (lower) simulated in the Control run. Units: 1/d.

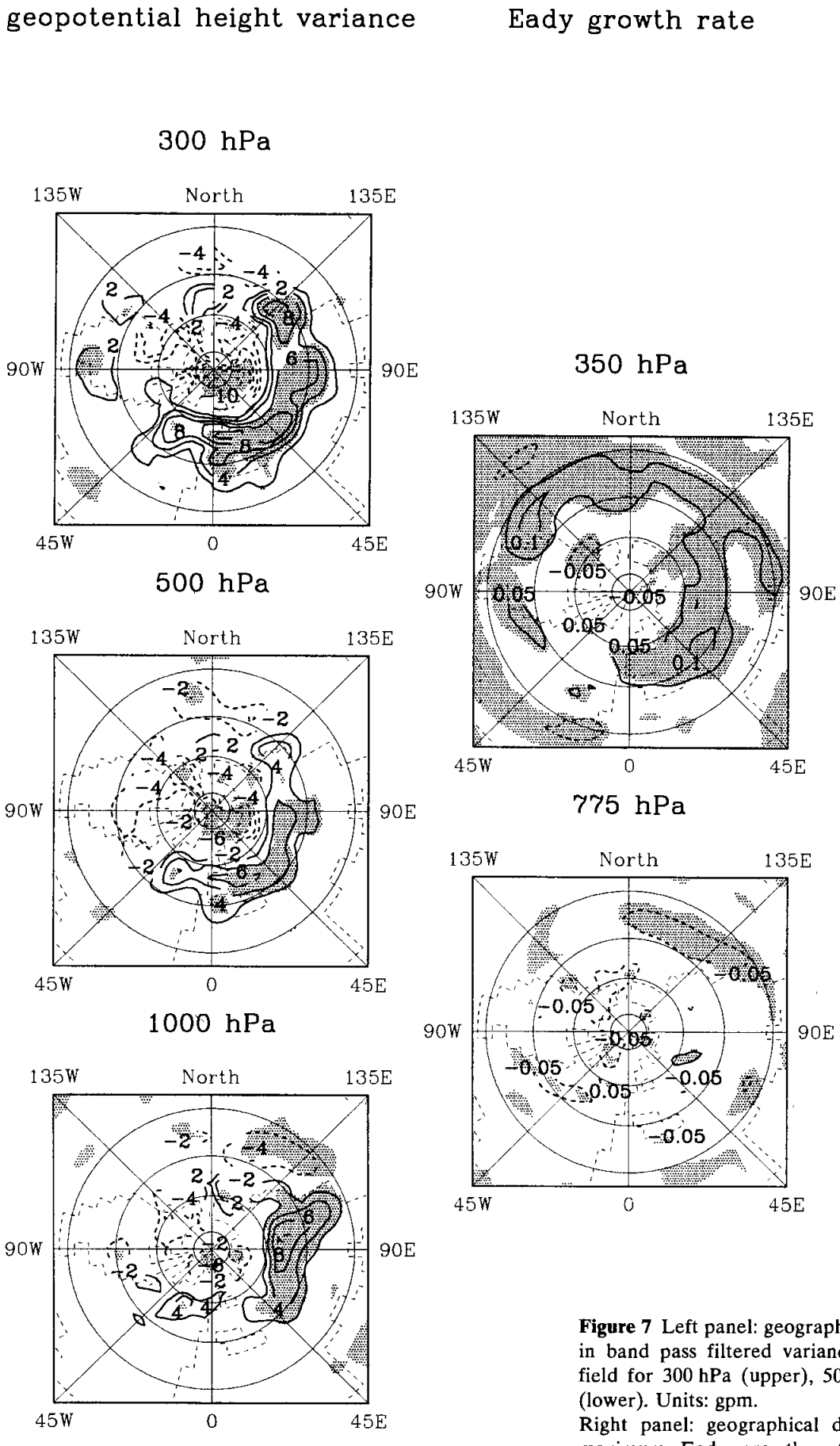

Figure 7 Left panel: geographical distribution of the change in band pass filtered variance of the geopotential height field for 300 hPa (upper), 500 hPa (middle) und 1000 hPa (lower). Units: gpm.
Right panel: geographical distribution of the change in maximum Eady growth rate for 350 hPa (upper) and 775 hPa (lower). Units: 1/d. Shaded areas denote statistical significance on the 95 % level.

experience strong intensification, are located upstream of the storm track maxima, which indicate high wave activity.

Figure 7, left panel, shows the differences in eddy activity between the Scenario A and the Control integrations. The most prominent signal with respect to the upper tropospheric (300 hPa) storm track is the intensification of eddy activity in an area extending from the eastern North Atlantic to Europe, and further over central Asia towards the Pacific coastline. This region of intensification thus stretches downstream from the maximum of the Atlantic storm track up to the area, where the Pacific storm track has its origin. The enhancement is statistically significant (95 %) over eastern Europe and parts of the Mediterranean, as well as over large parts of central and eastern Asia. Over the central North Pacific a slight, but statistically insignificant, attenuation and northward shift of the storm track at 300 hPa can be noticed .

The 500 hPa and 1000 hPa storm track signals reveal similar gross features as described for the upper troposphere. There are, however, remarkable differences between the three levels over Europe and the southern part of North America. The increase of activity over Europe at 300 hPa and 500 hPa is absent at 1000 hPa. Magnitude and extension of the signal at 500 hPa are generally less than at 300 hPa. At 1000 hPa, regions of significant intensification are shifted downstream relative to those aloft. Moreover, the attenuation and northward shift of the Pacific storm track are much more pronounced in the 1000 hPa level in comparison with the middle and upper levels.

In the case of the upper troposphere, regions which exhibit an intensification of the storm track are associated with a consistent increase of the baroclinic growth rate σ_{BI}. On the other hand, the increase in upper tropospheric σ_{BI} is not always associated with a corresponding signal in the stormtrack. Particularly, there are no clear and significant changes of the upper tropospheric storm track over the North Pacific, although values of σ_{BI} do increase. A pronounced and significant decrease of σ_{BI} is evident in the lower troposphere (775 hPa) for large parts of that region. This decrease is consistent with a local 1000 hPa storm track attenuation. In most other parts of the extratropics, only weak and insignificant decreases in lower-level σ_{BI} are notable, which have no correspondence to the stormtrack signals in the middle and lower troposphere. Our results show that stormtrack intensity changes cannot be regarded as a simple consequence of Eady growth rate changes at the respective level. The majority of the local anomalies can, however, be understood by taking into account that the typical development of baroclinic disturbances is not confined to particular levels but extends over the whole tropospheric column. In those regions where low-level baroclinicity remains basically unchanged, i.e. over most parts of the Atlantic and the Eurasian continent, low-level eddy activity changes are likely to be controlled by the remote effect of upper level baroclinicity changes. The upper tropospheric influence on eddy activity is, however, not evident if decreases of lower level baroclinicity are of substantial magnitude. These findings are not inconsistent with results obtained by Held and O'Brien (1992) and Pavan (1996) using β-channel models.

In conclusion, most of the storm track signal can be explained consistently by the Eady concept. The fact that not every detail completely fits into this concept is not a severe limitation. It rather hints at the necessity to consider additional processes such as local latent heat release.

4 Cyclone Frequency and Extreme Events

We will now discuss if there are indications of possible changes in the frequency and strength of weather extremes for the warmer climate. This question is closely connected with the response in cyclone activity. Cyclones do not only determine the mean distribution of precipitation and evaporation (i.e. the strength of the hydrological cycle) in mid-latitudes, but they are also the decisive synoptic feature connected with extreme events such as storms and floods.

So far we have made no clear distinction between cyclone activity and transient eddy activity, as diagnosed from bandpass-filtered geopotential height variance. It is well known, however, that the locations of maximum transient variability and the locations of maximum cyclone frequency do not necessarily coincide (e.g. König et al., 1993). As the changes of transient eddy activity are non-uniformly distributed over the northern hemisphere extratropics (Sections 2 and 3), we have to identify regions with intensified cyclonic activity before dealing with local changes of extreme events.

The changes of cyclonic frequency in the North Atlantic and North Pacific simulated by ECHAM2/OPYC are shown in Figure 8. The number of individual cyclones was calculated at each gridpoint

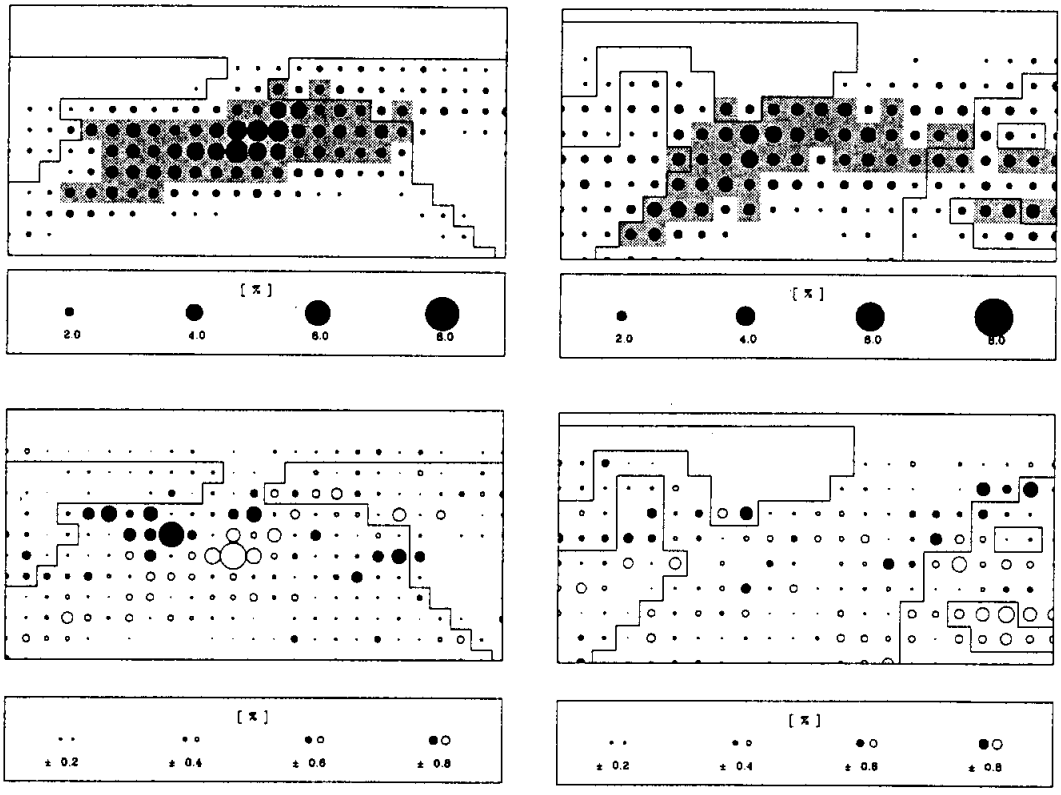

Figure 8 Upper pictures: Cyclone frequency for the North Pacific (left) and the North Atlantic (right) simulated in the Control run. Shaded areas denote values larger than 2 %. Lower pictures: Changes in cyclone frequency for the North Pacific (left) and the North Atlantic (right). Open circles denote negative values.

for the last ten winters of the Control and the Scenario A simulations using the objective method of König et al. (1993). In Figure 8 we present the relative cyclone frequencies (percentage of days at which a cyclone was located at the gridpoint under consideration) for the Control integration and the difference between Scenario A and Control. In the North Pacific, the main feature is a northwestward shift of cyclone frequency quite similar to the response of geopotential height variability (Figure 7; left panel). In the North Atlantic positive anomalies of cyclonic frequency can be noticed at the north-eastern edge of the North Atlantic cyclone track. These results are consistent with the analysis discussed in the previous section. No systematic spatial shift of the cyclone response with respect to the 1000 hPa transient variability response is present. It must be stressed at this point that most of the changes shown in Figure 8 are far from being statistically significant and should only be viewed as a supplementation to other results.

The problem of whether the most extreme events (i.e. these connected with catastrophe-like impacts) occur more frequently in a warmer climate cannot be discussed within the framework of a single 100 year transient Scenario experiment. Since only very few of these events are expected for a certain area (e.g. Europe) in a time scale of 100 years (1 or 2 say), differences between numbers of extraordinary events in 10 winter periods of the Scenario simulation and the Control run are meaningless as they could also be due to a sampling error. However, in order to shed some light on possible changes of the frequency of extreme events, the characteristics of European precipitation and near surface (10 m) windspeed simulated in the Scenario and the Control experiment have been studied. Europe was selected because the results reported above indicate that the Atlantic/European region is the most probable candidate for extreme value changes.

To assess changes of the frequency of extreme rainfall events, the space averaged (over all European land grid-points) daily rainfall is distributed into classes according to the associated precipitation rate. The classes are given by the intervals 0–1, 1–2, 2–3, ... mm/day. The relative number of days on which the rainfall lies within a certain class is calculated for the Control as well as for the Scenario A simulation. The histograms (Figure 9) indicate a distinct change in the distribution. While days with

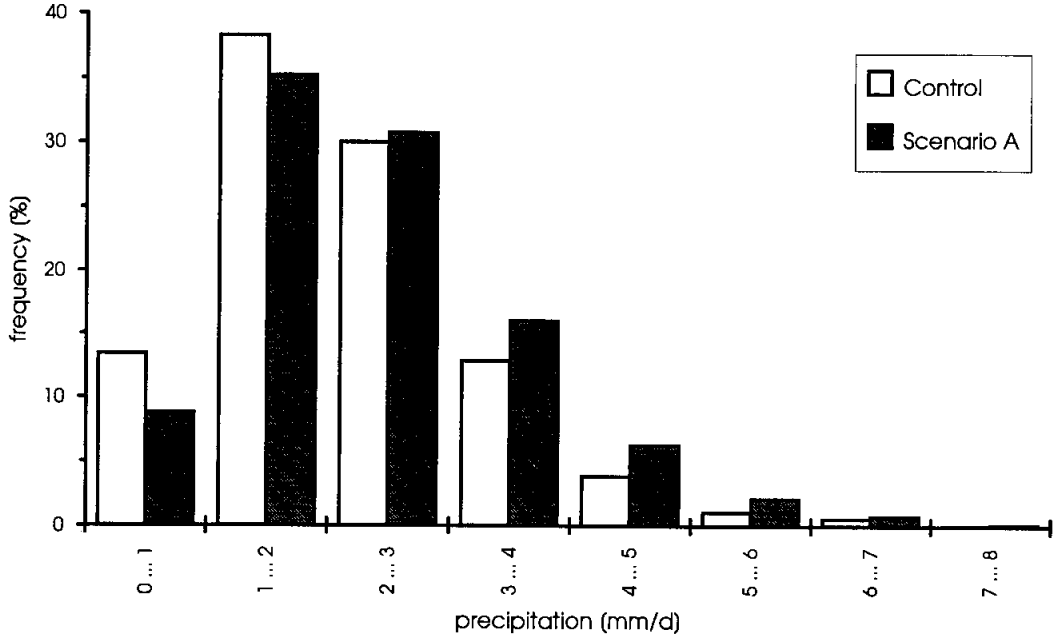

Figure 9 Percentage of days, for which the space averaged European daily precipitation lies within a certain range.

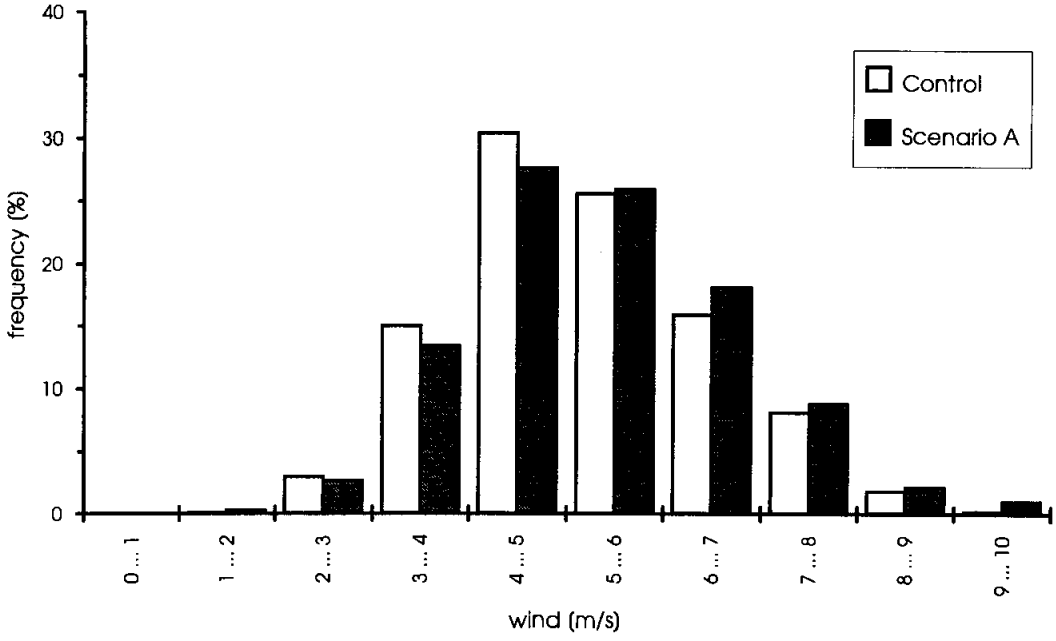

Figure 10 Percentage of days, for which the space averaged European daily near surface windspeed lies within a certain range.

1–2 mm/day rainfall occur most frequently in both simulations, their relative role is reduced in the Scenario A run. Instead, classes with more than 2 mm/day become more important. The time and space averaged European DJF precipitation only shows a slight increase from 2.1 mm/day to 2.4 mm/day.

A similar investigation was performed for the near surface (10 m) windspeed (Figure 10). Here we calculate the relative number of days, on which the space-averaged (again for all European land-points) windspeed is within a certain range (classes 0–1, 1–2, 2–3, ... m/s). In contrast to the precipitation, a slight decrease was found for the time and space average European windspeed from 5.0 m/s (Control) to 4.8 m/s (Scenario A). This is related to changes within the 4–5 m/s class. However, as for the precipitation, strong events occur more frequently

in the Scenario A simulation than in the Control run. The increasing occurence of high windspeeds and intense winter rains is consistent with the findings of Cubasch et al. (1995) and Gregory and Mitchell (1995), and also with the increased percentage of intense cyclones noted by Lambert (1995) and Carnell et al. (1996) for a warmer climate.

In summary, the extreme value changes are largely systematic in the European region and it seems justified to extrapolate the changes of the model distributions of precipitation and windspeed to those of the real world. An interpretation in this sense suggests that the probability of severe storms (even if these cannot be investigated with the present data) in the respective area will increase in a warmer climate. An estimation of quantitatively realistic extreme value changes, however, requires the application of atmospheric models with much higher resolution or the application of a specific regionalisation technique.

5 Conclusions

In order to determine potential changes of cyclonic activity in a warmer climate we have analysed data from a global coupled general circulation model applying a combination of several diagnostic tools. The diagnostic parameters were chosen to represent different scales relevant to cyclonic activity: the zonal mean structure of the global warming, the three-dimensional patterns of mid-latitude variability (storm tracks) and the related baroclinicity (measured in terms of the Eady growth rate) as well as local changes in cyclone frequency and the probability of extreme events. This procedure allows us to study, whether changes of the geographical distribution of cyclonic activity are consistently embedded in the full three-dimensional response of atmospheric fields.

One main result of the analysis is the highly non-uniform distribution of the changes in storm activity. An overall increase on the hemispheric scale, which one would expect by considering zonal averages only, does not occur, though more regions show indications towards an increase of storminess than towards a respective decrease. The Pacific storm track as one of the two major regions dominating northern hemisphere winter cyclonic activity does not seem to be very sensitive with respect to global warming, a fact that may be related to counteracting changes in upper and lower tropospheric baroclinicity. A northwestward shift is suggested but hardly a change of the mean intensity. In the Atlantic region, however, enhanced activity is clearly indicated, particularly at the eastern tail of the storm track. As the enhancement is accompanied by a northward shift of the storm track axis, more and (possibly) stronger cyclones are to be expected for western and northwestern Europe. These changes are also consistently linked to the probability of extreme events in Europe, where in the warmer climate stronger events of storminess and rainfall contribute more to the time average.

With few exceptions, the combined diagnostics results produce a consistent picture. Local changes, like the frequency of cyclones or extreme events, are reasonably related to changes of the three-dimensional large scale baroclinic structure. Therefore it is possible to put some reliability in localized features, even if they are not – themselves – statistically significant. Besides this internal consistency, our results (with respect to the North Atlantic storm track changes) also agree with those reported by other studies using a higher resolution (T42) atmospheric GCM and a mixed layer ocean (Hall et al., 1994) or a full dynamical ocean (Carnell et al., 1996). This coincidence of results from quite different model configurations may point to some degree of robustness and reliability.

Nevertheless some open questions remain: Firstly, we have considered moist effects only implicitly, i.e. as an inherent part of the simulations. The role of latent heat release in individual systems has not been quantified relative to the influence of changes in the three-dimensional temperature structure. Before assessing this question, we would have to validate the role of latent heat release for the life cycle of cyclones in our GCM and identify regions where local moist effects are of dominant importance. This requires the use of a number of additional diagnostic tools (like the three-dimensional distribution of diabatic heating) and is beyond the scope of this paper.

Secondly, we have not been able to explain the different response of the Pacific and the Atlantic storm tracks as a result of a global warming. It may be simply a consequence of the particular pattern of sea surface temperature and sea ice response. Another possibility is the potential difference in the dynamical mechanism controlling cyclonic activity in both areas. Deeper understanding in this respect would certainly help to improve our confidence in the GCM results.

Thirdly, in translating our results to the real world one has to keep in mind that the global warming pattern used here is associated with (equivalent) CO_2 increase. Additional forcings (e. g. from SO_4 aerosols) will certainly alter the basic temperature signal as well as the related cyclonic activity signal.

Finally, the coupled atmosphere-ocean GCM has some specific weaknesses, which are common to this generation of coupled models. A fully satisfactory interaction of the cyclonic and the planetary wave scale cannot be expected from a model of T21 horizontal resolution. The treatment of sea ice needs further improvement, too. Hence, even if our main results are largely coherent with those of other studies, it remains to be confirmed that the similarity of results arises from the same cause and effect relationships in the different models. For this purpose the combined application of various diagnostics, as proposed in this paper, may provide a particularly useful guideline for further analysis of the forthcoming generation of revised fully coupled atmosphere-ocean models at higher resolution.

Acknowledgements

This work was supported by the Bundesministerium für Bildung, Wissenschaft, Forschung und Technologie (BMBF) grants 07VKVO1/1, Nr. 6 and Nr. 25, and the European Union grants EV5V-CT92-0123 and ENV4-CT95-0102.

References

Blackmon, M. L., 1976: A Climatological Spectral Study of the 500 mb Geopotential Height of the Northern Hemisphere. J. Atmos. Sci. **33**, 1607–1623.

Carnell, R. E., C. A. Senior and J. F. B. Mitchell, 1996: An assessment of measures of storminess: Simulated changes in northern hemisphere winter due to increasing CO_2. Clim. Dyn. **12**, 467–476.

Chang, E. K. and I. Orlanski, 1993: On the Dynamics of a Storm Track. J. Atmos. Sci. **50**, 999–1015.

Cubasch, U., K. Hasselmann, H. Höck, E. Maier Reimer, U. Mikolajewicz, B.D. Santer and R. Sausen, 1992: Time-dependent greenhouse warming computations with a coupled ocean atmosphere model. Clim. Dyn. 8, 55–69.

Cubasch, U., J. Waszekewitz, G. Hegerl and J. Perlwitz, 1995: Regional climate changes as simulated in time-slice experiments. Climatic Change **31**, 273-304.

Deutscher Bundestag, 1991: Protecting the earth: a status report with recommendations for a new energy policy. Bonn: Referat Öffentlichkeitsarbeit, ISBN 3-924521-71-9.

Flohn, H., A. Kapala, H. R. Knoche and H. Mächel, 1992: Water vapor as an amplifier of the greenhouse effect: new aspects. Meteorol. Zeitschrift N.F. **1**, 122–138.

Gregory, J. M. and J. F. B. Mitchell, 1995: Simulation of daily variability of surface temperatures and precipitation over Europe in the current and $2 \times CO_2$ climates using the UKMO climate model. Q.J.R. Meteorol. Soc. **121**, 1451–1476.

Hall, N. M. J., B. J. Hoskins, P. J. Valdes and C. A. Senior, 1994: Storm tracks in a high resolution GCM with doubled CO_2. Q.J.R. Meteorol. Soc. **120**, 1209–1230.

Hall, N. M. J., B. Dong and P. J. Valdes, 1996: Atmospheric equilibrium, instability and energy transport at the last glacial maximum. Clim. Dyn. **12**, 497–511.

Held, I. M., 1993: Large scale dynamics and global warming. Bull. Am. Met. Soc. **74**, 228–241.

Held, I. M. and E. O'Brien, 1992: Quasigeostrophic turbulence in a Three-Layer-Model: Effects of vertical structure in the mean shear. J. Atmos. Sci. **49**, 1961–1870.

Hoskins, B. J. and P. Valdes, 1990: On the existence of storm tracks. J. Atmos. Sci. **47**, 1854–1864.

Houghton, J. J., B. A. Callander and S. K. Varney, 1992: Climate changes 1992. The supplementary report to the IPCC assessment. Cambridge University Press, Cambridge, 138 pp.

Houghton, J. J., L. G. Meiro Filho, B. A. Callander, N. Harris, A. Kattenberg and K. Maskell, 1996: Climate Change 1995. The science of climate change. Cambridge University Press, Cambridge, 584 pp.

König W., R. Sausen and F. Sielmann, 1993: Objective identification of cyclones in GCM simulations. J. Climate **6**, 2217–2231.

Lambert, S. J., 1995: The effect of enhanced greenhouse warming on winter cyclone frequencies and strengths. J. Climate **8**, 1447–1452.

Lindzen, R. S. and B. Farrell, 1980: A simple approximate result for maximum growth rate of baroclinic instabilities. J. Atmos. Sci. **37**, 1648–1654.

Lunkeit, F., R. Sausen and J. M. Oberhuber, 1996a: Climate simulations with the global coupled atmosphere-ocean model ECHAM2/OPYC, Part I: present day climate and ENSO events. Clim. Dyn. **12**, 195–212.

Lunkeit, F., R. Sausen and J. M. Oberhuber, 1996b: Climate simulations with the global coupled atmosphere-ocean model ECHAM2/OPYC, Part II: a greenhouse warming scenario. In preparation.

Manabe, S., R. J. Stouffer, M. J. Spelman and K. Bryan, 1991: Transient response of a coupled ocean-atmosphere model to gradual changes of atmospheric CO_2. Part I: annual mean response. J. Climate **4**, 785–818.

Mitchell, J. F. B.,S. Manabe, T. Tokioka and V. Meleshko, 1990: Equilibrium climate change. In Climate Change – the IPCC scientific assessment. Houghton, J. T., G. J. Jenkins and J. J. Ephraums (Eds.). Cambridge University Press.

Murphy, J. M. and J. F. B. Mitchell, 1995: Transient response of the Hadley Centre coupled ocean-atmosphere model to increasing carbon dioxide. Part II: Spatial and temporal structure of response. J. Climate **38**, 57–80.

Oberhuber, J. M., 1993a: Simulation of the Atlantic circulation with a coupled sea-ice-mixed layer-isopycnical general circulation model. Part I: Model description. J. Phys. Oceanogr. **23**: 808–829.

Oberhuber J. M., 1993b: Simulation of the Atlantic circulation with a coupled sea-ice-mixed layer-isopycnical general circulation model. Part II: Model experiment. J. Phys. Oceanogr. **23**: 830–845.

Pavan, V., 1996: Sensitivity of a multi-layer, quasi-geostrophic β-channel to the vertical structure of the equilibrium meridional temperature gradient. Q.J.R. Meteorol. Soc. **122**, 55–72.

Ponater M., W. König, R. Sausen and F. Sielmann, 1994: Circulation regime fluctuations and their effect on intraseasonal variability in the ECHAM climate model. Tellus **46A**, 265–285.

Roeckner, E., K. Arpe, L. Bengtsson, S. Brinlcop, L. Dümenil, M. Esch, E. Kirk, F. Lunkeit, M. Ponater, B. Rockel, R. Sausen, U. Schlese, S. Schubert and M. Windelband, 1992: Simulation of the present-day climate with the ECHAM model: Impact of model physics and resolution. Max-Planck-Institut für Meteorologie, Report No. **93**, ISSN 0937-1060.

Senior, C. A., 1995: The dependence of climate sensitivity on the horizontal resolution of a GCM. J. Climate **8**,2860–2880.

Siegmund, P. C., 1990: The effect of a doubling of atmospheric CO_2 on the storm tracks in the climate of a general circulation model. Royal Netherlands Meteorological Institute internal report.

Stephenson, D. B. and I. M. Held, 1993: GCM response of northern winter stationary waves and storm tracks to increasing amounts of carbon dioxide. J. Climate **6**, 1859–1870.

Wilson, C. A. and J. F. B. Mitchell, 1987: A doubled CO_2 climate sensitivity experiment with a global climate model including a simple ocean. J. Geophys. Res. **92**, 13315–13343.